LETTER

https://doi.org/10.1038/s41586-018-0598-9

Battery-operated integrated frequency comb generator

Brian Stern[1,2], Xingchen Ji[1,2], Yoshitomo Okawachi[3], Alexander L. Gaeta[3] & Michal Lipson[2]*

Optical frequency combs are broadband sources that offer mutually coherent, equidistant spectral lines with unprecedented precision in frequency and timing for an array of applications[1]. Frequency combs generated in microresonators through the Kerr nonlinearity require a single-frequency pump laser and have the potential to provide highly compact, scalable and power-efficient devices[2,3]. Here we demonstrate a device—a laser-integrated Kerr frequency comb generator—that fulfils this potential through use of extremely low-loss silicon nitride waveguides that form both the microresonator and an integrated laser cavity. Our device generates low-noise soliton-mode-locked combs with a repetition rate of 194 gigahertz at wavelengths near 1,550 nanometres using only 98 milliwatts of electrical pump power. The dual-cavity configuration that we use combines the laser and microresonator, demonstrating the flexibility afforded by close integration of these components, and together with the ultra low power consumption should enable production of highly portable and robust frequency and timing references, sensors and signal sources. This chip-based integration of microresonators and lasers should also provide tools with which to investigate the dynamics of comb and soliton generation.

Frequency combs based on chip-scale microresonators offer the potential for high-precision photonic devices for time and frequency applications using a highly compact and robust platform. By pumping the microresonator with a single-frequency pump laser, additional discrete, equidistant frequencies are generated through parametric four-wave mixing (FWM), resulting in a Kerr frequency comb[2,4–7]. Under suitable conditions temporal cavity solitons can be excited, which results in stable, low-noise combs with ultraprecise spacing[8–13]. Many applications require such tight frequency and timing stability, including spectroscopy[14–16], low-noise microwave generation[17], photonic frequency synthesis[18], optical clocks[19], distance ranging[20,21] and telecommunications[22].

Although one of the most compelling advantages for microresonator combs is the potential for the pump source and the microresonator to be fully integrated, previous demonstrations using integrated resonators have relied on external pump lasers that are typically large, expensive and power-hungry, preventing applications where size, portability and low power consumption are critical. Power-efficient integrated lasers have been developed using silicon laser cavities with bonded or attached III–V materials to provide optical gain[23–26], but losses in these silicon waveguides make comb generation impractical at low power. On the other hand, silicon nitride (Si_3N_4) microresonators were recently demonstrated with record low parametric oscillation thresholds[27] due to the high quality factors ($Q > 3 \times 10^7$), high nonlinear refractive index ($n_2 \approx 2.4 \times 10^{-19}$ m^2 W^{-1}) and small mode volume (ring radius approximately 100 μm). Additionally, owing to the high index of refraction of Si_3N_4 ($n \approx 2.0$) and its low loss, compact, tunable Si_3N_4 laser cavities with narrow linewidth have been demonstrated[28,29]. Si_3N_4 is a common complementary metal oxide semiconductor (CMOS)-compatible deposited material that can be fabricated at wafer scale, and the combination of efficient comb generation and available integration of active devices make it an ideal platform for complete integration of optical frequency combs.

Here we demonstrate a Kerr comb source on an integrated hybrid III–V/Si_3N_4 platform, using a compact, low-power, electrically pumped source. In our approach (Fig. 1), a gain section based on a III–V reflective semiconductor optical amplifier (RSOA) is coupled to a Si_3N_4 laser cavity, which consists of two Vernier microring filters for wavelength tunability and a high-Q nonlinear microresonator (Fig. 1b). The nonlinear microresonator serves two purposes. First, it generates a narrowband back-reflection due to coupling between counter-propagating circulating beams resulting from Rayleigh scattering[30], effectively serving as an output mirror of the pump laser cavity, as we previously demonstrated[28]. Second, the microresonator generates a frequency comb through parametric FWM. In this way, the comb generation and pump laser are inherently aligned, a configuration that was previously explored using resonators in fibre laser cavities with fibre amplifiers[31,32]. Integrating the comb source with the laser allows the flexibility to use such a configuration, avoiding the typical chain of discrete components found in all previous Kerr comb demonstrations. Figure 1c shows the assembled millimetre-sized comb source, which has only electrical inputs and an optical output (see Methods for fabrication details).

We designed the Si_3N_4 laser cavity to ensure tunable, single-mode lasing and provide sufficient pump output power for comb generation in the nonlinear microresonator. The lasing wavelength is controlled by the alignment of the two microring Vernier filters[25], which are in turn aligned with one of the modes of the larger microresonator shown in Fig. 1b. The filters' radii are 20 μm and 22 μm, corresponding to free spectral ranges (FSRs) of 1.18 THz and 1.07 THz, respectively, which result in transmission at only a single frequency when the filters are aligned. Their resonance positions can be widely tuned using integrated resistive microheaters, as shown in Fig. 2a. The filters' transmission bandwidth is designed to have a full-width at half-maximum of 15 GHz by ensuring strong coupling to the two adjacent waveguides with a 5 μm coupling length. The optical gain in the laser cavity comes from electrical pumping of the III–V waveguide on the RSOA, which is coupled to the Si_3N_4 cavity at one end and strongly reflects at the opposite end (see Methods). The output coupler of the laser cavity is a 120-μm-radius microresonator with a measured reflection of 40% on resonance, as shown in Fig. 2b. This level of reflection allows for high laser output power due to the high round-trip gain of the RSOA. The measured transmission spectrum of the microresonator (Fig. 2b) corresponds to an intrinsic Q of $(8.0 \pm 0.8) \times 10^6$. Based on this Q and the anomalous group-velocity dispersion for the 730 nm× 1,800 nm waveguide, simulations indicate that a soliton-state frequency comb can be generated with 700 μW of pump power in the bus waveguide just before the microresonator (Extended Data Fig. 1).

We find lasing with up to 9.5 mW output optical power using the integrated Si_3N_4 laser. In order to characterize the laser, we first operate the microresonator slightly detuned from resonance to ensure that only

[1]School of Electrical and Computer Engineering, Cornell University, Ithaca, NY, USA. [2]Department of Electrical Engineering, Columbia University, New York, NY, USA. [3]Department of Applied Physics and Applied Mathematics, Columbia University, New York, NY, USA. *e-mail: ml3745@columbia.edu

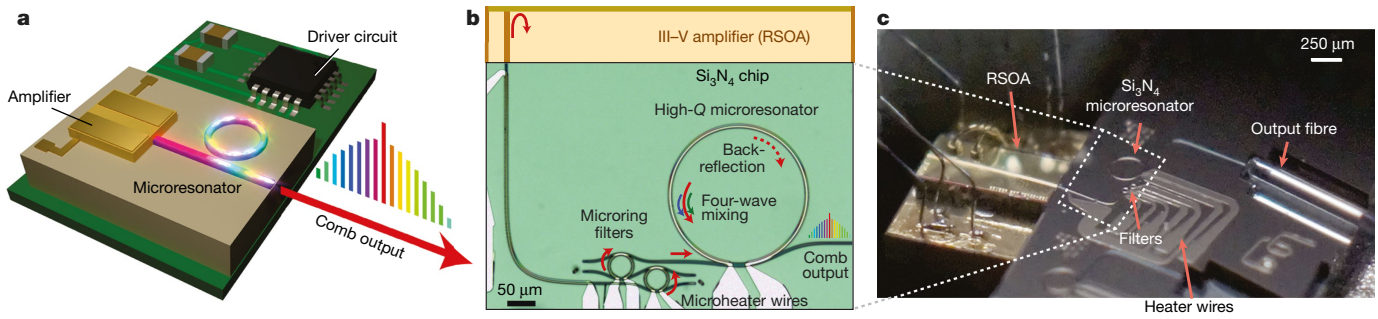

Fig. 1 | Integrated frequency comb source. a, The concept of an integrated Kerr comb source with an on-chip amplifier and microresonator. **b**, Microscope image and diagram of the integrated comb source, including the laser cavity and the high-Q nonlinear microresonator for comb generation. The reflective III–V semiconductor optical amplifier (RSOA) waveguide provides electrically pumped optical gain and includes a reflective facet on one end (top), while the opposite side is coupled to the Si_3N_4 portion of the laser cavity. The microring filters and the larger microresonator are tunable using integrated microheaters. The latter generates a partially reflected beam to form a second effective mirror of the laser cavity. This microresonator also has a high Q to enable FWM and comb generation. **c**, Photograph of the integrated comb source. The RSOA is edge-coupled to the Si_3N_4 chip and supplied with electric current via wires, while the comb output is measured using an optical fibre.

lasing occurs and a frequency comb is not generated. We observe lasing with a side-mode suppression ratio (SMSR) of more than 60 dB (Fig. 2c). As shown in Fig. 2d, the lasing threshold is 49 mA, with a slope efficiency of 52 mW A^{-1}. The maximum on-chip output power of 9.5 mW is obtained at 277 mW (220 mA) electrical pump power consumption, P_{elec}. This corresponds to a 3.4% wall-plug efficiency (that is, output optical power divided by electrical power). Additionally, we measure a narrow laser linewidth of 40 kHz using the delayed self-heterodyne method (see Methods). The relatively high output power and narrow linewidth are competitive with those of many bulk pump lasers, yet the present laser is much more compact.

Using our cavity design, we generate a Kerr comb spanning more than 8 THz and achieve a mode-locked, single-soliton state with P_{elec} less than 100 mW, enabling battery-operation applications. We observe new optical frequencies beginning to appear adjacent to the 1,579 nm pump owing to FWM in the microresonator once the laser power measured after the ring (P_{opt}) reaches a threshold of 1.1 mW at $P_{elec} = 78$ mW. We then increase P_{elec} above threshold to 130 mW and monitor comb formation as the microresonator is tuned using its integrated microheater (see Methods for the set-up and tuning procedure). When the microresonator is first detuned slightly, we measure $P_{opt} = 2.5$ mW for the single lasing mode (Fig. 3a). As the microresonator is tuned into resonance, greater circulating power leads to comb

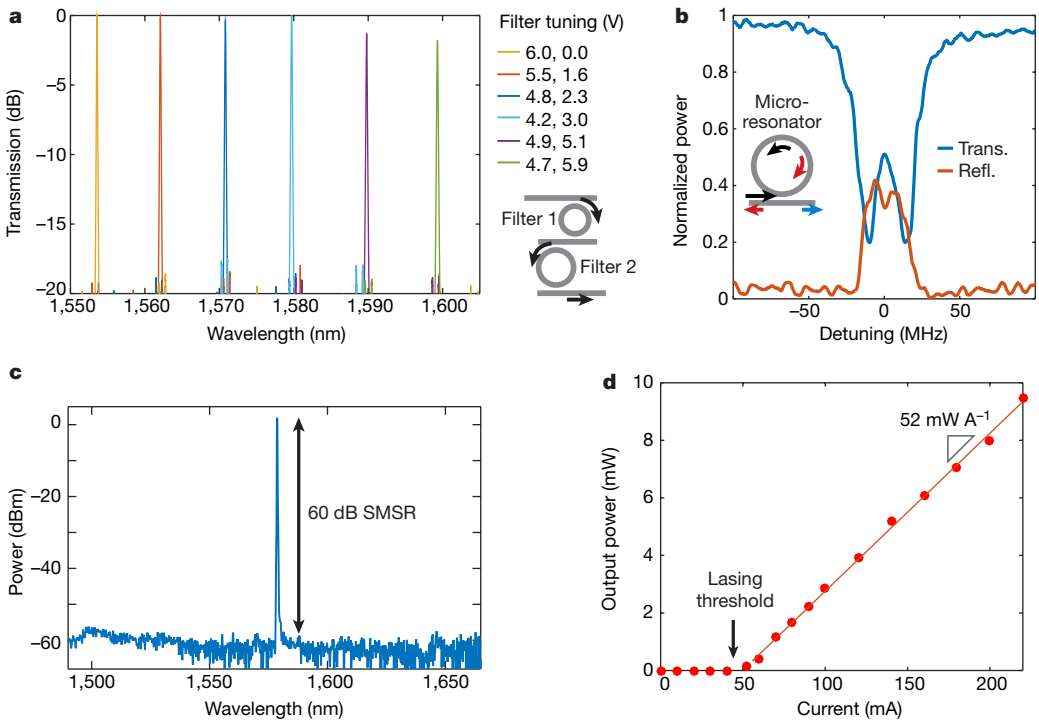

Fig. 2 | Characterization of the integrated III–V/Si_3N_4 laser. a, Measured transmission spectra (normalized) for the Vernier filter microrings (filter 1 and filter 2, diagram at right). By adjusting the voltage applied to the microheaters, the filters' relative detuning is adjusted and a single transmission wavelength is selected. Key at right shows voltage applied in the format 'filter 1, filter 2'. **b**, Measured optical transmission and reflection spectra (normalized) of the high-Q microresonator. The 32-MHz resonance bandwidth reveals a Q of 8×10^6. The narrowband reflection is generated by coupling via Rayleigh scattering between counter-propagating beams in the ring (arrows show beam directions, colour code as spectra), which is apparent due to the resonance splitting observed from these degenerate beams. **c**, Laser output spectrum at 85 mA showing single-mode lasing with a side-mode suppression ratio (SMSR) of more than 60 dB. **d**, Output optical power of laser versus pump current at 1,580 nm with a slope efficiency of 52 mW A^{-1}.

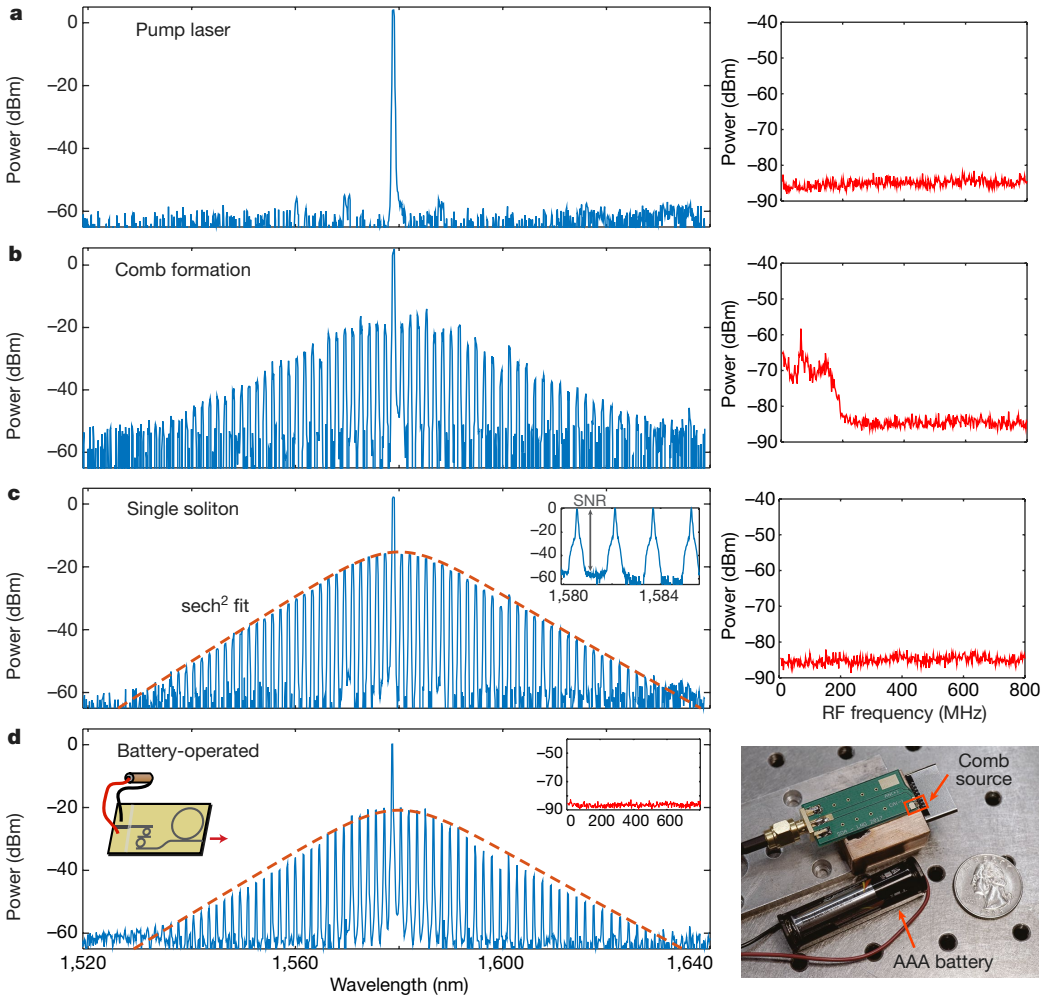

Fig. 3 | Generation of mode-locked soliton frequency combs. **a**–**c**, Left, spectra of output from the comb source as measured by an optical spectrum analyser at varying stages of comb generation; right, corresponding RF spectra (resolution bandwidth 100 kHz). A current supply provides electrical pump power of 130 mW. **a**, Spectrum of the laser output before tuning fully into resonance. The RF noise is low since there is only single-frequency lasing. **b**, Spectrum of the frequency comb. Because the comb is not yet mode-locked, beating between different comb lines produces high RF noise below 200 MHz. **c**, Single-soliton frequency comb spectrum with the characteristic sech profile (see Extended Data Fig. 2). Inset, the signal-to-noise ratio (SNR, grey vertical arrow) is approximately 50 dB; variables plotted on the axes are the same as in the main panel. The comb linewidth is separately measured as 40 kHz (see Methods). The RF spectrum confirms the transition to a low-noise state. **d**, Left panel, frequency comb spectrum matching soliton sech profile generated with an AAA battery supplying pump power of 98 mW. Left inset, diagram of battery operated device, showing filters 1 and 2 (see Fig. 2a) and the microresonator (large circle). Right inset, RF spectrum showing low-noise state; *y* axis, power in dBm, *x* axis, RF frequency in MHz. Right panel, photograph of integrated comb source (shown boxed in red) with a printed circuit board and the battery (arrowed) next to a US quarter for scale.

formation, accompanied by high radio frequency (RF) noise (Fig. 3b). Tuning the resonance further results in stable combs with smooth spectral envelopes characteristic of temporal cavity solitons[8]. We measure a single-soliton state with a 8.6 THz (72 nm) 30-dB bandwidth accompanied by a drop in RF noise (Fig. 3c). Once generated, the soliton exhibits stable behaviour without feedback electronics or temperature control, with no visible changes in the optical spectrum or output power until the microresonator is intentionally detuned. The power of the comb lines totals 0.24 mW, indicating that a higher effective pump power may be resulting from our placement of the microresonator in the laser cavity. Such efficient operation allows us to also show battery-operation of the comb source by supplying the pump current using a standard AAA battery. At $P_{elec} = 98$ mW from the battery, we measure $P_{opt} = 1.3$ mW and a comb matching the single-soliton profile (Fig. 3d). These results represent unprecedented low-power consumption for generating Kerr frequency combs and solitons with an integrated microresonator.

In order to show the versatility of this platform, we demonstrate a more traditional but still laser-integrated configuration in which the comb is generated in a microresonator that is distinct from the pump laser. In this second design, shown in Fig. 4a, the Vernier filters and RSOA function in the same way as in the first design, but a Sagnac loop mirror is now included to serve as the output coupler with approximately 20% reflection. Because this mirror has a broadband reflection, tunable lasing can take place independent of the resonance position of the comb microresonator. With the microresonator fully off-resonance, we measure single-mode lasing at 1,582 nm with $P_{opt} = 4.9$ mW and over 60 dB SMSR (Fig. 4b) at $P_{elec} = 162$ mW. By tuning the microresonator into resonance with the laser wavelength, we can generate a frequency comb (Fig. 4c). Through further tuning of the resonance (see Methods), we observe a multiple-soliton-state frequency comb spanning a 13.4 THz (105 nm) 30-dB bandwidth with the characteristic drop in RF noise (Fig. 4d). We model a two-soliton-state comb and obtain a profile closely matching that of the experimental comb (Fig. 4d). Single-soliton combs should also be achievable with this configuration, but in this device we only observed two or more solitons. Multiple-soliton combs in microresonators have been used previously to demonstrate dual-comb spectroscopy, for example[16]. The measured comb power is 80 μW, corresponding to a conversion efficiency of 1.6%. The comb power scales with the number of solitons, as does the number

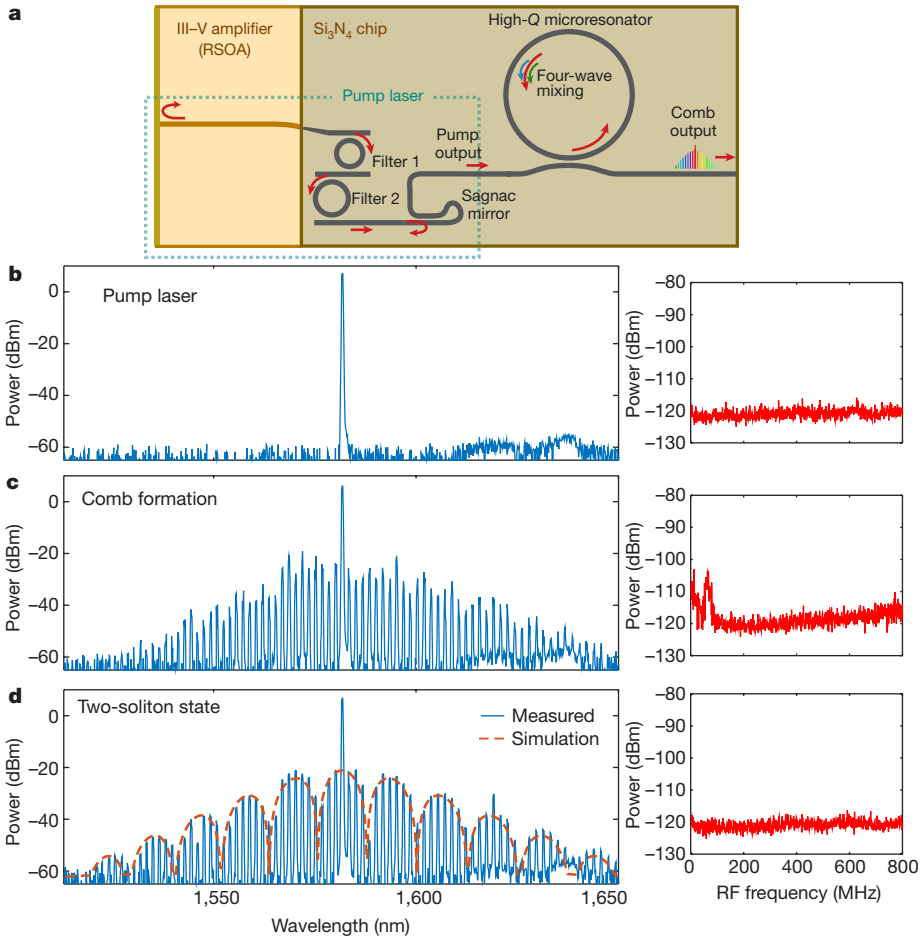

Fig. 4 | Modular configuration of the integrated comb source. **a**, Schematic of the modular comb source configuration. Here the integrated laser (turquoise dashed box) is distinct from the nonlinear microresonator, with a Sagnac loop mirror serving as the laser output coupler. The arrows show the path of light travelling through the laser cavity and reflecting back at the reflective end (left) of the RSOA and at the Sagnac mirror, with the laser output partially transmitting through the latter. **b**–**d**, Optical output spectra at varying stages of comb generation (left panel) with corresponding RF spectra (right panel; resolution bandwidth 100 kHz). **b**, Spectrum of laser output. The RF noise is low because there is only single-frequency lasing. **c**, Spectrum of frequency comb before mode-locking with associated high RF noise. **d**, Spectrum of two-soliton frequency comb. The RF spectrum confirms the low-noise state.

of pulses per round-trip. In Methods, we discuss the relative advantages of the two designs.

This demonstration of a laser-integrated Kerr comb source presents opportunities in many fields that rely on the precision and stability of frequency combs and solitons, including sensing, metrology, communications and waveform generation. The low power consumption of our platform enables these applications in a battery-powered and mobile system without the need for external lasers, moveable optics, or laboratory set-ups. Our platform is CMOS-compatible for wafer-scale fabrication of robust integrated photonic chips, potentially enabling wide deployment of precision devices, such as portable spectrometers for molecular sensing[14,15] or vehicle-mounted systems for distance ranging[20,21]. In future implementations, the RSOA could be placed directly on the silicon substrate, through passively aligned mounting[25] or material bonding[23], taking advantage of the infrastructure for assembly and packaging of III–V and silicon chips that is already scaled to mass production for silicon photonic transceivers. Additional photonic components such as filters for wavelength-division multiplexing[22] or waveguide couplers for mixing multiple combs[14,15,18] could also be placed on-chip to combine frequency combs with more complex integrated photonic circuits.

Online content

Any methods, additional references, Nature Research reporting summaries, source data, statements of data availability and associated accession codes are available at https://doi.org/10.1038/s41586-018-0598-9.

Received: 30 March 2018; Accepted: 8 August 2018;
Published online 8 October 2018.

1. Newbury, N. R. Searching for applications with a fine-tooth comb. *Nat. Photon.* **5**, 186–188 (2011).
2. Del'Haye, P. et al. Optical frequency comb generation from a monolithic microresonator. *Nature* **450**, 1214–1217 (2007).
3. Pasquazi, A. et al. Micro-combs: a novel generation of optical sources. *Phys. Rep.* **729**, 1–81 (2018).
4. Jung, H., Xiong, C., Fong, K. Y., Zhang, X. & Tang, H. X. Optical frequency comb generation from aluminum nitride microring resonator. *Opt. Lett.* **38**, 2810–2813 (2013).
5. Savchenkov, A. A. et al. Tunable optical frequency comb with a crystalline whispering gallery mode resonator. *Phys. Rev. Lett.* **101**, 093902 (2008).
6. Levy, J. S. et al. CMOS-compatible multiple-wavelength oscillator for on-chip optical interconnects. *Nat. Photon.* **4**, 37–40 (2010).
7. Razzari, L. et al. CMOS-compatible integrated optical hyper-parametric oscillator. *Nat. Photon.* **4**, 41–45 (2010).
8. Herr, T. et al. Temporal solitons in optical microresonators. *Nat. Photon.* **8**, 145–152 (2014).
9. Saha, K. et al. Modelocking and femtosecond pulse generation in chip-based frequency combs. *Opt. Express* **21**, 1335–1343 (2013).
10. Yi, X., Yang, Q.-F., Yang, K. Y., Suh, M.-G. & Vahala, K. Soliton frequency comb at microwave rates in a high-Q silica microresonator. *Optica* **2**, 1078–1085 (2015).
11. Yu, M., Okawachi, Y., Griffith, A. G., Lipson, M. & Gaeta, A. L. Mode-locked mid-infrared frequency combs in a silicon microresonator. *Optica* **3**, 854–860 (2016).
12. Xue, X. et al. Mode-locked dark pulse Kerr combs in normal-dispersion microresonators. *Nat. Photon.* **9**, 594–600 (2015).
13. Volet, N. et al. Micro-resonator soliton generated directly with a diode laser. *Laser Photonics Rev.* **12**, 1700307 (2018).

14. Suh, M.-G., Yang, Q.-F., Yang, K. Y., Yi, X. & Vahala, K. J. Microresonator soliton dual-comb spectroscopy. *Science* **354**, 600–603 (2016).
15. Dutt, A. et al. On-chip dual-comb source for spectroscopy. *Sci. Adv.* **4**, e1701858 (2018).
16. Yu, M. et al. Silicon-chip-based mid-infrared dual-comb spectroscopy. *Nat. Commun.* **9**, 1869 (2018).
17. Liang, W. et al. High spectral purity Kerr frequency comb radio frequency photonic oscillator. *Nat. Commun.* **6**, 7957 (2015).
18. Spencer, D. T. et al. An optical-frequency synthesizer using integrated photonics. *Nature* **557**, 81–85 (2018).
19. Papp, S. B. et al. Microresonator frequency comb optical clock. *Optica* **1**, 10–14 (2014).
20. Suh, M.-G. & Vahala, K. J. Soliton microcomb range measurement. *Science* **359**, 884–887 (2018).
21. Trocha, P. et al. Ultrafast optical ranging using microresonator soliton frequency combs. *Science* **359**, 887–891 (2018).
22. Marin-Palomo, P. et al. Microresonator-based solitons for massively parallel coherent optical communications. *Nature* **546**, 274–279 (2017).
23. Fang, A. W. et al. Electrically pumped hybrid AlGaInAs-silicon evanescent laser. *Opt. Express* **14**, 9203–9210 (2006).
24. Van Campenhout, J. et al. Electrically pumped InP-based microdisk lasers integrated with a nanophotonic silicon-on-insulator waveguide circuit. *Opt. Express* **15**, 6744–6749 (2007).
25. Kobayashi, N. et al. Silicon photonic hybrid ring-filter external cavity wavelength tunable lasers. *J. Lightwave Technol.* **33**, 1241–1246 (2015).
26. Lee, J.-H. et al. Demonstration of 12.2% wall plug efficiency in uncooled single mode external-cavity tunable Si/III-V hybrid laser. *Opt. Express* **23**, 12079–12088 (2015).
27. Ji, X. et al. Ultra-low-loss on-chip resonators with sub-milliwatt parametric oscillation threshold. *Optica* **4**, 619–624 (2017).
28. Stern, B., Ji, X., Dutt, A. & Lipson, M. Compact narrow-linewidth integrated laser based on a low-loss silicon nitride ring resonator. *Opt. Lett.* **42**, 4541–4544 (2017).
29. Oldenbeuving, R. M. et al. 25 kHz narrow spectral bandwidth of a wavelength tunable diode laser with a short waveguide-based external cavity. *Laser Phys. Lett.* **10**, 015804 (2013).
30. Liang, W. et al. Whispering-gallery-mode-resonator-based ultranarrow linewidth external-cavity semiconductor laser. *Opt. Lett.* **35**, 2822–2824 (2010).
31. Pasquazi, A. et al. Self-locked optical parametric oscillation in a CMOS compatible microring resonator: a route to robust optical frequency comb generation on a chip. *Opt. Express* **21**, 13333–13341 (2013).
32. Johnson, A. R. et al. Microresonator-based comb generation without an external laser source. *Opt. Express* **22**, 1394–1401 (2014).

Acknowledgements We are grateful to S. Miller, C. Joshi, T. Lin, U. Dave and J. Jang for discussions and to M. Yu for help with soliton simulations. We also thank M. C. Shin and O. Jimenez for packaging advice. This work was supported by AFRL programme award number FA8650-17-P-1085; the ARPA-E ENLITENED programme (DE-AR0000843); the Defense Advanced Research Projects Agency (DARPA) under the Microsystems Technology Office Direct On-Chip Digital Optical Synthesizer (DODOS) program (N66001-16-1-4052) and the Modular Optical Aperture Building Blocks (MOABB) programme (HR0011-16-C-0107); the STTR programme (N00014-16-P-30); and the Air Force Office of Scientific Research (AFOSR) (FA9550-15-1-0303). X.J. acknowledges the China Scholarship Council for financial support. This work was performed in part at the Cornell NanoScale Facility, an NNCI member supported by NSF grant ECCS-1542081.

Reviewer information *Nature* thanks W. Freude and the other anonymous reviewer(s) for their contribution to the peer review of this work.

Author contributions B.S. conceived the work, designed and assembled the devices, performed the measurements, and prepared the manuscript. X.J. fabricated the devices. B.S. and X.J. characterized the microring transmission. Y.O. simulated the soliton combs. M.L. and A.L.G. supervised the project. All authors discussed the results and edited the manuscript.

Competing interests All authors are listed as inventors in a patent application related to this work, filed by Columbia University.

Additional information
Extended data is available for this paper at https://doi.org/10.1038/s41586-018-0598-9.
Reprints and permissions information is available at http://www.nature.com/reprints.
Correspondence and requests for materials should be addressed to M.L.
Publisher's note: Springer Nature remains neutral with regard to jurisdictional claims in published maps and institutional affiliations.

METHODS

Fabrication. The Si_3N_4 devices are fabricated[27] by first growing 4 μm of SiO_2 on a crystalline silicon wafer using thermal oxidation to form the bottom cladding of the waveguides. Then 730 nm of Si_3N_4 is deposited using low pressure chemical vapour deposition (LPCVD). The wafer is annealed in two stages to remove hydrogen impurities. The waveguides are then patterned using electron beam lithography and etched using CHF_3 plasma etching. The waveguides are clad with 2 μm SiO_2. The microheaters are placed over the waveguides using 100 nm of sputtered platinum (with a titanium adhesion layer) and lift-off patterning.

RSOA/Si_3N_4 coupling and electrical connection. The III–V RSOA gain chip used here is commercially available from Thorlabs (SAF 1126) and provides broad gain near 1,550 nm. One side has 93% reflection and the other side is anti-reflection coated. This second side is coupled to the Si_3N_4 chip with the waveguides angled relative to the facets to further prevent reflections[28]. The Si_3N_4 chip is polished up to the end of a tapered 280-nm-wide waveguide which is simulated to have less than 1 dB coupling loss to the mode of the RSOA waveguide. The two chips are attached and aligned using three-axis stages with micrometers. We measure an experimental 2 dB coupling loss. The RSOA is wirebonded to an electrical printed circuit board (PCB) for supplying the pump current from either a Keithley 2400 SourceMeter or an AAA battery with a tunable potentiometer. The microheaters of the Si_3N_4 chip are connected to pads and interfaced with a DC wedge probe (GGB Industries) and controlled by a DAC (Measurement Computing) supplying about 30 mW to each heater. The Si_3N_4 waveguide output is formed as an inverse-taper to edge-couple to a lensed single-mode fibre.

Laser set-up and comb generation procedure. In order to reach mode-locked soliton combs in the first configuration, which uses the dual-cavity design, we first calibrate the laser by aligning the resonances of the two Vernier microring filters using the integrated heaters. This may be done by monitoring the transmitted amplified spontaneous emission (ASE) noise through the filters from the RSOA or by using a separate laser to calibrate the wavelength tuning. Next, the nonlinear microresonator is tuned using its heater to align to the filters' resonances. Once the three are aligned with the pump current above threshold, the device begins to lase. The cavity phase shifter heater, which is positioned over a section of waveguide between the filters and the RSOA, is then tuned to maximize the output power, and the filters may again be adjusted slightly to maximize the output.

After this initialization procedure, the resonance of the nonlinear microresonator is tuned to a longer wavelength such that the original lasing mode is blue-detuned and lasing ceases because the microresonator is no longer on resonance to provide the back-reflection as the laser's output mirror. From this point, the heater is tuned back in the opposite direction to blue-shift the resonance and go through the stages of Fig. 3a–c: first lasing, then chaotic comb generation, and finally soliton states[33]. The resonance producing soliton states corresponds to an effectively red-detuned laser[8], where the detuning results in a typical pump-to-comb conversion efficiency of several per cent[34]. With further tuning of the resonance, output power begins to drop and eventually lasing ceases once the microresonator is fully detuned from the filters and the cavity mode. This procedure allows repeatable generation of soliton states by tuning at rates up to about 10 kHz using a function generator applying a triangle wave voltage to the heater, as shown previously by Joshi et al.[33]; however, we are also often able to reach the soliton states by manual tuning of the heater voltage without a function generator. This relative ease of mode-locking is likely to be a feature of the self-aligning dual-cavity configuration.

In the second, modular configuration, the soliton generation procedure is identical to the first, with the exception that lasing may take place with the nonlinear microresonator off-resonance, allowing a simpler calibration set-up but without the inherent alignment of the microresonator. In both configurations, we were alternatively able to tune the laser from shorter to longer wavelengths across the microresonator resonance using the cavity phase shifter and also achieve soliton mode-locked combs.

Owing to the low pump power needed to generate frequency combs in the microresonator, we did not observe significant thermal shifts in the resonance. If scaled to higher powers where such shifts become stronger, the speed of the resonance tuning can be adjusted to match the power dissipation in the soliton state[8,33].

While we did not require active feedback to maintain the soliton state during our experiments (timescales up to an hour), future systems could account for environmental fluctuations using active feedback[35] to stabilize the soliton states indefinitely. This feedback and the initialization procedure could potentially be controlled using a low-power microcontroller integrated alongside the photonic chip (Fig. 1a) implementing pulse width modulation to efficiently tune the heaters[36].

Comparison of the designs. The two designs demonstrated here, consisting of a dual-cavity comb source and a traditional modular configuration, enable new flexibility in designing the pump laser for generating the frequency comb. The dual-cavity configuration ensures that the microresonator is inherently aligned with the laser because the feedback reflection completes the laser cavity[37]. Detuning the microresonator is still possible, but we observed lower sensitivity to the exact heater settings than found in the modular design, allowing for easier tuning into soliton mode-locked combs through manual tuning (although the automated tuning procedure above was successfully applied to both designs). Additionally, this first design showed a strong output comb power relative to the pump output. Because the microresonator is part of the laser cavity, we cannot directly measure the pump power input to the microresonator, but the theoretical conversion efficiency for solitons[34] suggests that the effective pump input may be notably stronger than the pump output after the microresonator.

The comb generation process in the second, modular design is directly analogous to most previous Kerr comb experiments[8,10,33,38,39]. Despite the potential advantages of the first design, the traditional approach may be desirable if the pump laser and microresonator need to be discretely controlled rather than tuned together. For example, the laser may be locked to a stable reference at a fixed wavelength, simplifying the tuning controls—only the microresonator need be tuned.

Laser and comb linewidth measurement. The laser linewidth is measured using the delayed self-heterodyne method[28]. The laser output at 80 mA pump current is sent to an interferometer with one path delayed by 12 km of fibre (corresponding to a delay of 58 μs). The other path is phase modulated at 300 MHz. The resulting beat signal is measured on an electrical spectrum analyser (Agilent E4407B) and a 40 kHz Lorentzian linewidth is determined.

The comb linewidth is measured by beating a single comb line with a 1,560 nm 2.4 kHz-linewidth reference laser (Redfern Integrated Optics). With a pump current of 120 mA, a single soliton comb is generated (as in Fig. 3c), and the output is sent to a 50:50 coupler, with the other input coming from the reference laser followed by a polarization controller. The heterodyne output is sent to a photodiode and the RF beat note corresponds to the comb linewidth, which we measure to be approximately 40 kHz, matching that of the pump laser.

Data availability

The data that support the findings of this study are available from the corresponding authors on reasonable request.

33. Joshi, C. et al. Thermally controlled comb generation and soliton modelocking in microresonators. *Opt. Lett.* **41**, 2565–2568 (2016).
34. Bao, C. et al. Nonlinear conversion efficiency in Kerr frequency comb generation. *Opt. Lett.* **39**, 6126–6129 (2014).
35. Yi, X., Yang, Q.-F., Yang, K. Y. & Vahala, K. Active capture and stabilization of temporal solitons in microresonators. *Opt. Lett.* **41**, 2037–2040 (2016).
36. Cong, G. W. et al. Power-efficient gray-scale control of silicon thermo-optic phase shifters by pulse width modulation using monolithically integrated MOSFET. In *Optical Fiber Communication Conference (2015) M2B.7* (Optical Society of America, 2015).
37. Peccianti, M. et al. Demonstration of a stable ultrafast laser based on a nonlinear microcavity. *Nat. Commun.* **3**, 765 (2012).
38. Hausmann, B. J. M., Bulu, I., Venkataraman, V., Deotare, P. & Lončar, M. Diamond nonlinear photonics. *Nat. Photon.* **8**, 369–374 (2014).
39. Webb, K. E., Erkintalo, M., Coen, S. & Murdoch, S. G. Experimental observation of coherent cavity soliton frequency combs in silica microspheres. *Opt. Lett.* **41**, 4613–4616 (2016).

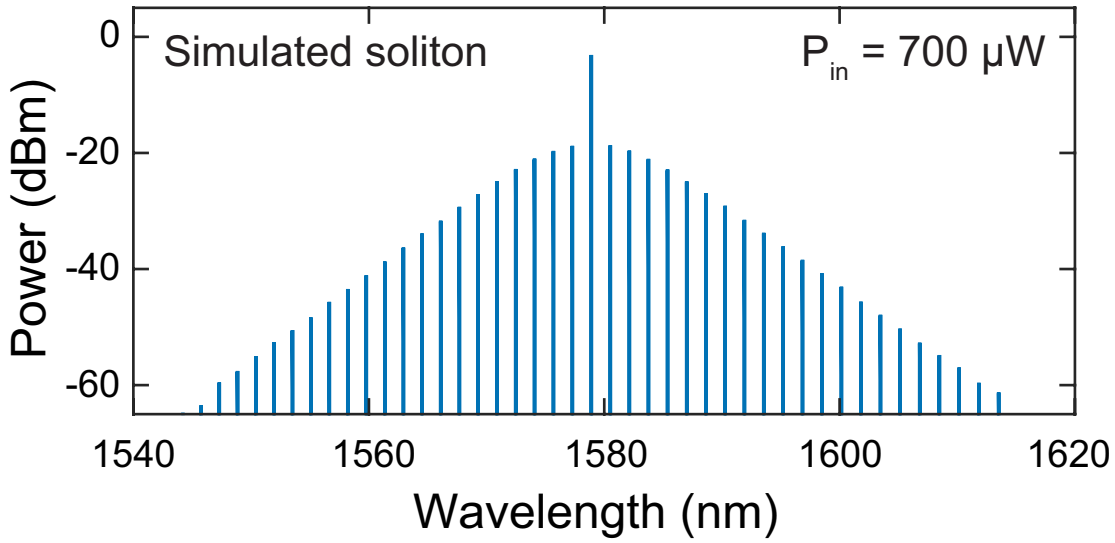

Extended Data Fig. 1 | Comb generation simulation at low optical power. Shown is the simulated optical spectrum of a soliton comb generated with 700 μW optical pump power (P_{in}) in the bus waveguide before the microresonator. The microresonator dimensions used in the model are 730 nm × 1,800 nm with a radius of 120 μm, corresponding to a 194 GHz FSR.

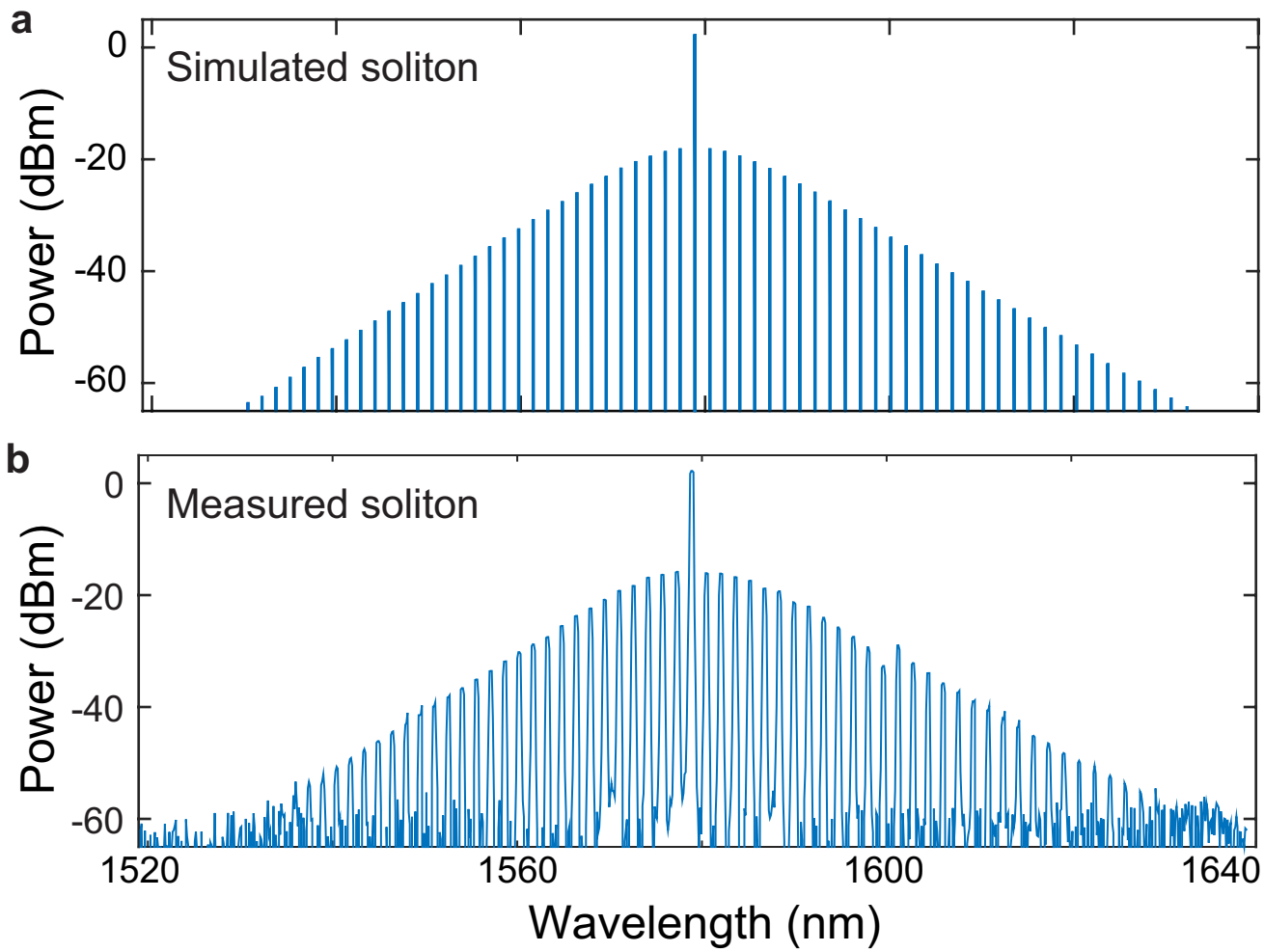

Extended Data Fig. 2 | Comparison of simulated and measured solitons. **a**, Simulation of a single-soliton comb generated with 2 mW optical pump power in the bus waveguide before the microresonator (1.66 mW after the microresonator). The microresonator dimensions used in the model are 730 nm × 1,800 nm with a radius of 120 μm, corresponding to a 194 GHz FSR. **b**, Optical spectrum of a measured single-soliton comb (from Fig. 3c) with 1.66 mW pump power in the bus waveguide after the microresonator. The sech profile and comb bandwidth qualitatively match those of the simulated comb.